Optimization of Phase-Engineered a-Si:H-Based Multijunction Solar Cells

C. R. Wronski, R. W. Collins, J. M. Pearce, J. Deng, V. Vlahos, G. M. Ferreira, and C. Chen
Center for Thin Film Devices
The Pennsylvania State University, University Park, PA 16802

ABSTRACT

A comprehensive understanding is being developed on the subjects of Si:H material deposition as well as device limiting mechanisms. First, it has been demonstrated that the protocrystalline nature of the p-layers *and not their microcrystalline nature* is responsible for obtaining high V_{OC} and also that V_{OC} can be maximized through the deposition procedure. Second, recombination at p/i interfaces has been identified and quantified on cells with different i-layers and a-Si:H p-i interface layers. The bulk recombination in both the J_D-V and J_{SC}-V_{OC} characteristics, which exhibit superposition, is found to be consistent with the Shockley-Reed-Hall model, and the observed spatially uniform distributions of defects in the i-layers are contrary to the predictions of the defect pool model. Third, results obtained on sub-bandgap absorption *spectra* have identified two distinctly different defects located at 1.0 and 1.2eV from the conduction band. The evolution of these defects under light induced degradation depends on the microstructure of the a-Si:H.

1. Introduction

The objectives of this research are to develop and characterize monolayer scale processes of hydrogenated silicon (Si:H) film growth in order to improve further solar cell performance and stability. In order to improve materials and devices prepared at high deposition rates, a comprehensive understanding is being developed with respect to materials growth and device limiting mechanisms. Such an understanding involves: the development of phase diagrams for both intrinsic and doped protocrystalline materials; characterization of the properties of different a-Si:H thin film materials; reliable correlation of cell characteristics with bulk i-layer properties requiring quantitative evaluations of contributions from interfaces; and finally, a better understanding of the Staebler-Wronski Effect (SWE). Some of the results obtained in these studies are briefly reviewed here.

2. Deposition Phase Diagrams

Using real time spectroscopic ellipsometry (RTSE) to characterize thin film growth and microstructure, we have shown that the thin film Si:H prepared under moderate-to-high H_2-dilution conditions evolves from the "protocrystalline" amorphous phase to a mixed [amorphous + microcrystalline] phase [(a+μc)-Si:H] with accumulated thickness of the layer [1]. Consequently, without using RTSE, or equally powerful techniques, it is not possible to control the growth of the protocrystalline Si:H materials and cell structures or to characterize their properties reliably.

A key capability of RTSE is the ability to generate deposition phase diagrams for different hydrogen dilution ratios, R, and different substrate materials [2]. These diagrams identify the ranges of thickness over which it is possible to obtain the pure protocrystalline phase as well as the ranges corresponding to the mixed-phase for a given set of deposition conditions. Such insights have been applied successfully to phase engineering of solar cell structures for optimum performance [3]. Phase diagrams have also been developed for rf PECVD deposition processes in order to achieve high deposition rates. The approach for characterization of such evolving films and cell structures applied here is unlike any reported previously for solar cells incorporating i-layers prepared with H_2-dilution, since in the previous work clearly present phase transition regions are neither separated nor characterized in any meaningful way.

Phase diagrams have also been successful in explaining the nature of p-type Si:H films doped with BF_3 and in guiding the development of high V_{OC} in n-i-p solar cells [4]. It has been proposed for a long time that the optimum p-layers are high conductivity doped microcrystalline Si:H (μc-Si:H). We find this earlier work unconvincing and conclude that the protocrystalline nature of the p-type Si:H layers -- *and not their microcrystalline nature* -- is responsible for obtaining high V_{OC} in n-i-p a-Si:H solar cells. Using RTSE, phase diagrams plotted as a function of $R = [H_2]/[SiH_4]$ were obtained that describe the microstructural evolution with thickness for protocrystalline p-layers having different doping gas flow ratios $D = [BF_3]/[SiH_4]$.

Figure 1 shows the extended phase diagram for the deposition of p-type Si:H with D = 0.2 on an amorphous Si:H film, a substrate similar to that incorporated into the n-i-p cell structure. The doping level was set at D = 0.2 in order to achieve high conductivity in both the single-phase μc-Si:H films and the protocrystalline Si:H films. The phase diagram shows two transitions, one occurring from amorphous to mixed-phase Si:H [a→(a+μc)] and the other occurring from mixed-phase to single-phase microcrystalline Si:H [(a+μc)→μc]. From this phase diagram, it can be seen that the protocrystalline Si:H doped layer obtained at R = 150 (solid vertical arrow) is amorphous throughout growth to a thickness of 200 Å whereas, in contrast, at R=200 the p-layer grows as mixed phase Si:H immediately and coalesces to single-phase μc-Si:H after 200 Å.

The results obtained from this phase diagram, can be directly related to the measurements performed on corresponding n-i-p solar cells using R=10 i-layers and

200Å D = 0.2 p-layers, also shown in Figure 1. The results show that the optimum p-layers for obtaining high V_{OC} are clearly within the protocrystalline Si:H growth regime. The protocrystalline nature of these p-layers as determined by RTSE was also confirmed with AFM and TEM measurements. It can be seen from these results that in order to maximize V_{OC}, it is necessary to deposit the p-layer at the maximum R value that allows the desired thickness to be obtained without crossing the transition into the mixed amorphous + microcrystalline phase growth regime.

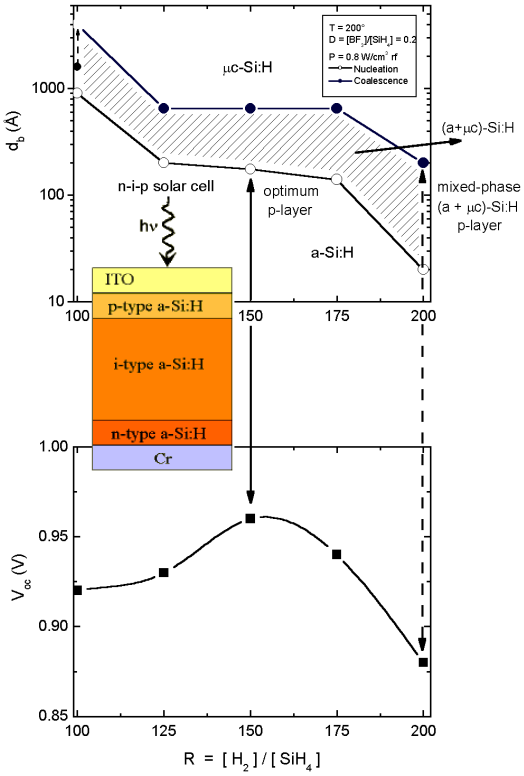

Figure 1. The extended phase diagram depicting the bulk thickness (Å) as a function of R for p-type Si:H deposition with D=0.2 on a-Si:H substrates at 200°C; also shown is V_{OC} (V) as function of R for solar cells with the corresponding 200Å p-layers.

3. Device Loss Mechanisms

Several issues have been addressed in this research regarding the mechanisms and defects determining a-Si:H solar cell characteristics that have not been clearly resolved in previous studies. These include: (i) identifying and then quantifying the contributions to carrier recombination occurring at the interfaces and in the bulk of the i-layers; (ii) assessing the serious consequences that result when interpreting solar cell characteristics based on the assumption of spatially non-uniform distributions of defects in the i-layers as predicted by the defect thermodynamics model [5]; and (iii) correlating carrier recombination to different cell characteristics self consistently. Studies addressing these issues were carried out applying the forward bias dark current (J_D–V) characteristics of both p-i-n (superstrate) and n-i-p (substrate) solar cell structures. These structures were prepared using p a-SiC:H with different a-Si:H interface i-layers and R = 0, R = 10 intrinsic bulk layers having thicknesses from 0.2 to 1.5 μm. By controlling the recombination at the p/i interfaces through changes the band gap of the 200 Å a-Si:H i-layers adjacent to the a-SiC:H p-contact, it was possible to separate clearly the contributions to the J_D–V characteristics of the intrinsic layers from those of the p/i interfaces. In fact, systematic changes are obtained in the J_D–V characteristics of the cell structures with R=0 and R=10 i-layers. Figure 2 shows the results on p-i-n cell structures with 4000 Å R = 10 i-layers and 200Å p/i interface layers consisting of R = 0, R = 10 and R = 40 a-Si:H. Similar systematic changes in the J_D–V characteristics are also obtained with the cells having R = 0 i-layers.

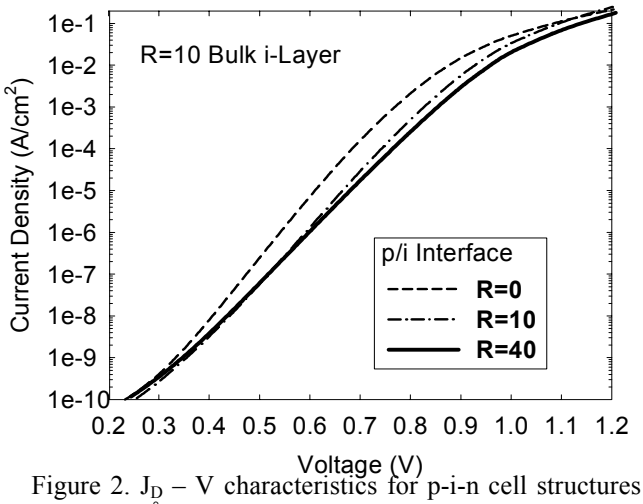

Figure 2. J_D – V characteristics for p-i-n cell structures with 4000 Å R = 10 a-Si:H i layers and R = 0, 10 and 40 a-Si:H at the p/i interfaces.

The type of dependence of J_D on V associated with recombination at the p/i interfaces can be seen with an R = 0 layer at the p/i interface whose large recombination exhibits an effective diode quality factor m* of ~1.2. The effects of reducing this recombination results in the dramatically different J_D–V characteristics whereby the bulk contributions can now be identified. Extended regions with an effective diode quality factor m of ~1.4 are present, clearly indicating that these currents are due to carrier recombination in the bulk. Such bulk recombination -- and the voltage range over which it is present -- could be further confirmed by the increases in J_D and changes resulting from the introduction of light induced bulk defects.

The J_D–V characteristics corresponding to the bulk and the m values of cells having i-layers with both R = 10 and R = 0 can be shown to be consistent with the Shockley-Reed-Hall (SRH) model [6], whereby recombination occurs through *spatially uniform densities of defects* having a continuous distribution in the gap. Further evidence for such uniform distributions of defects in the i-layer and the absence of the high densities of defects in the interface regions as predicted by the defect pool model was obtained from results on cells with i-layers of different thickness as

well as results on superstrate (p-i-n) and substrate (n-i-p) cell structures.

A consequence of the large defect densities at the interfaces (as predicted by the defect pool model) is that they should dominate carrier recombination in the i-layers and so there should be no dependence of the J_D-V characteristics on i-layer thickness. The "elusive" dependence of J_D–V characteristics on thickness [7] was in fact obtained in cell structures with both R = 0 and R = 10 i-layers. A systematic *increase* in the bulk recombination currents can be clearly observed as the i-layer thicknesses are increased together with a *decrease* in the corresponding far forward bias currents expected when the transport ceases to be diffusion/recombination and becomes drift dominated [8].

In the case of the p-i-n and n-i-p cell structures, equivalence is found between the measured J_D-V characteristics, considering cells having different i-layers and p/i interfaces. These results are in conflict with the defect pool model that predicts that the very high densities of defects adjacent to the p/i and n/i interfaces, depend on the sequence in which the p and n layers are deposited. This prediction would lead to significant differences in the J_D-V characteristics between the two cell structures.

In view of the above results, *homogeneous distributions of defects* in the i-layers of the a-Si:H solar cells are clearly established, whereas those predicted by the defect pool model are ruled out. As a result, the properties of the cell that are clearly identified and confirmed as those associated with the bulk i-layer in fact can be directly correlated with the properties of the corresponding i-layer films.

The goal of self consistently correlating carrier recombination between different cell characteristics has been achieved by comparing the J_D-V characteristics with those of J_{SC}-V_{OC} in the different cell structures. The reported absence of superposition between the two characteristics [9] in the past has been attributed to the large differences in the nature of carrier recombination occurring in the dark and under illumination. In all the cells studied here superposition is found between J_D-V and J_{SC}-V_{OC} over extended regions of voltage and illumination, as expected from the SRH recombination mechanism. This is illustrated in Figure 3 with the characteristics of one of the cell structures in the annealed state and after nine hours of illumination with red light.

Figure 3 shows that in the annealed state excellent superposition exists between J_{SC}–V_{OC} and J_D–V characteristics from 0.2V to 0.7V and for currents up to ~10^{-4} A/cm^2. The range of this superposition after degradation, however, reduces to 0.6 V and 10^{-6} A/cm^2. From both first principle arguments and computer simulations, it can be shown that the split between the J_{SC}–V_{OC} and J_D–V in the higher voltage region is due to the fact that dark current injection is limited by the barriers at the p/i and n/i interfaces. This is reflected in the observation that the J_{SC}–V_{OC} characteristic remains in an exponential regime whereas the J_D–V does not. The space charge at the interface regions associated with the n and p contacts, that results from the defects in the i-layer, act as current limiting barriers at high forward bias. Unlike the built-in junction barrier across the bulk, the barriers formed by the p and n contacts are not lowered by the forward bias, and the carrier concentrations at the contacts remain essentially constant with forward bias. The results obtained after degradation with volume absorbed red light in Figure 3 confirm the argument that the field distortion induced by such space charge causes a split of the J_{SC}–V_{OC} and J_D–V characteristics.

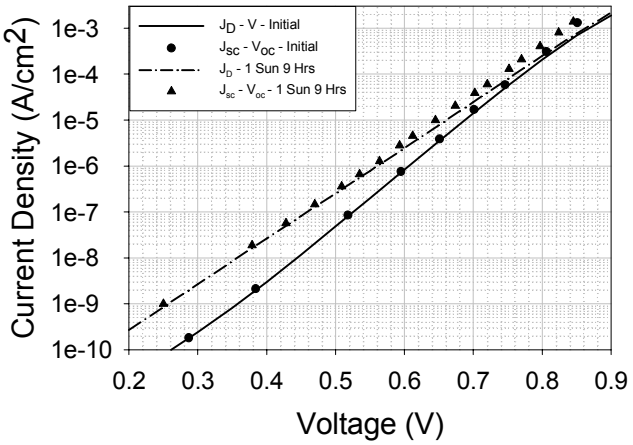

Figure 3. J_{sc} – V_{oc} and J_D – V characteristics of a p-i-n cell with an R=10 4000Å i layer and an R=40 p/i interface both before and after degradation with 1 sun of red light.

4. Staebler Wronski Effect

Degradation of cells and corresponding intrinsic films carried out under 1 sun illumination at different temperatures clearly exhibit kinetics that cannot be fit with a single rate equation as has been carried out extensively in the past [10, 11]. Direct correlations have been found between the electron mobility lifetimes ($\mu\tau$) and fill factors, but no such agreements could be found with the magnitude of subgap absorption $\alpha(E)$ [10, 11]. The absence of such a simple correlation is a consequence of the fact that the evolution of the different light induced defects during degradation is reflected not only in the magnitude of $\alpha(E)$ but also in the shape of $\alpha(E)$ [10]. Consequently detailed studies have been undertaken to identify and characterize the evolution of the different light induced defects from the *spectra* of $\alpha(E)$ obtained with dual beam photoconductivity measurements on materials with different microstructures. The evolution of the defect states and their energy distribution is obtained from $\alpha(E)$, which is proportional to $\int N(E)N_{CO}(E+h\upsilon-E_C)^{1/2}dE$. $N(E)$ is the energy dependent density of gap states, $N_{CO}(E-Ec)^{1/2}$ is the parabolic distribution of extended states in the conduction band, and $h\upsilon$ is the incident photon energy in the subgap absorption measurement that excites electrons from the gap states into the conduction band [12].

The creation by light of distinctly different defects near midgap, as well as below, has been deduced from the derivatives of $\alpha(E)$ normalized to those in the annealed state. An example of this behavior is illustrated in Figure 4 for 1 sun degradation at 25°C and 75°C for a protocrystalline film

deposited with hydrogen diluted with silane at R=10, and for one deposited at a high rate (20 Å/s) without hydrogen dilution. Figure 4 shows the dα/dE spectra at the two temperatures for the protocrystalline R=10 film in the degraded steady state and for the undiluted 20 Å/s film after 30 hours of 1 sun illumination. These dα(E)/dE results reflect the changes in N(E) of the gap states since the states in the conduction band do not change upon illumination. It can be seen clearly in Figure 4(a) that upon illumination of the R=10 film, the increase in N(E) occurs predominantly for gap states centered around 1.0 eV from the conduction band.

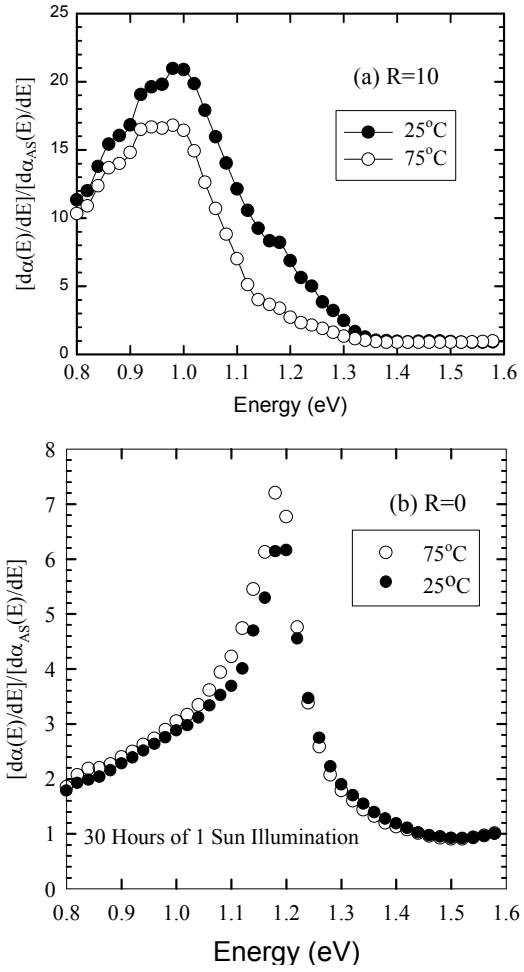

Figure 4. The derivatives of the subgap absorption degraded at 25°C and 75°C normalized to those in the annealed state for (a) R=10 material in the 1 sun degraded steady state and (b) R=0 20 Å/s material after 30 hours of 1 sun illumination

In Figure 4 (b) on the other hand, this increase is clearly centered around 1.2eV. In addition, one can see the large effects of the microstructure for the two materials, as well as differences in the nature of their defects.

At the higher temperature the creation of states around 1.2 eV is suppressed in Figure 4(a), whereas in Figure 4(b) there is virtually no change in the light induced gap states created after 30 hours of illumination. It should be pointed out also that these results for N(E) are directly reflected in the corresponding results for the electron mobility – lifetimes. In the case of the protocrystalline material there is a corresponding increase in the electron-mobility products by a factor of ~2 between 25°C and 75°C whereas in the undiluted 20 Å/s material they remain virtually the same.

Studies on materials having different microstructures are currently being correlated with the deconvolution of gap states derived from the changes in bulk recombination currents obtained from J_D-V and J_{SC}-V_{OC} characteristics.

5. Acknowledgements

The authors acknowledge support for this work from the National Renewable Energy Laboratory under Subcontract No. NDJ-2-30630-01.

REFERENCES

[1] H. Fujiwara, J. Koh, C. R. Wronski, and R. W. Collins, *Appl. Phys. Lett.* **70**, 2150, 1997.

[2] A. S. Ferlauto, R. J. Koval, C. R. Wronski, and R. W. Collins, *Appl. Phys. Lett*. **80,** 2666, 2002.

[3] R. J. Koval, J. M, Pearce, A. S. Ferlauto, P. I. Rovira, R. W. Collins, and C. R. Wronski, *Proceedings of the 28th IEEE PV Specialists Conference. Proc*., (IEEE 2000), p. 750, 2000.

[4] R. J. Koval, C. Chen, G. M. Ferreira, J. M. Pearce, C. R. Wronski, and R. W. Collins, *Appl. Phys*. Lett. **81**, 1258, 2002.

[5] H. M. Branz and R. S. Crandall, *Solar Cells* **27**, 159, 1989.

[6] W. Shockley and W. T. Read, *Phys. Rev*. **87**, 835, 1952.

[7] M. A. Kroon and A. C. Van Swaaij, *J. Appl. Phys*. **90**, 994, 2001.

[8] K. Lips, *Mat. Res. Soc. Symp. Proc*. **37**, 455, 1995.

[9] S. S. Hegedus, N. Salzman, and E. Fagan, *J. Appl. Phys*. **63**, 1526, 1988.

[10] J. Pearce, X. Niu, R. Koval, G. Ganguly, D Carlson, R. W. Collins, and C. R. Wronski, *Mat. Res. Soc. Symp. Proc*. **664**, A12.3, 2001.

[11] C. R. Wronski, J. M. Pearce, R. J. Koval. X. Niu, A. S. Ferlauto, J. Koh, R. W. Collins, *Mat. Res. Soc. Symp. Proc*. **715**, A13.4, 2002.

[12] L. Jiao, I. Chen, R. W. Collins, C. R. Wronski, and N. Hata, *Appl. Phys. Lett*. **72**, 1057, 1998.